CROATICA CHEMICA ACTA
CCACAA **81** (2) 369–379 (2008)

ISSN-0011-1643
CCA-3254
Conference Paper

Structural Analysis of a Series of Copper(II) Coordination Compounds and Correlation with their Magnetic Properties

Bojan Kozlevčar* and Primož Šegedin

Faculty of Chemistry and Chemical Technology, University of Ljubljana, Aškerčeva 5, P. O. Box 537, SI-1001 Ljubljana, Slovenia

RECEIVED NOVEMBER 6, 2007; REVISED JANUARY 10, 2008; ACCEPTED JANUARY 16, 2008

Keywords
copper(II)
structure
EPR
magnetism
carboxylates
lignin

The chemistry of copper(II) is widely described in the literature due to its importance in various fields of research and because of the relative ease in the synthesis of new compounds. The magnetochemistry is one of these fields. However the results obtained with 'the magnetic methods' *e. g.* EPR and magnetic susceptibility, that may enable important insight in the properties of the compounds, are very often ambiguous. The structural correlation of the wide range of copper(II) complexes with the magnetic analysis can fulfil some gaps in this area. A series of copper(II) complexes, synthesized in our lab during the last decade, is discussed.

INTRODUCTION

A structural diversity of the copper(II) complexes is largely related to a Cu^{II} d^9 system. It enables a variety of coordination polyhedra with significantly different geometries. Copper(II) is found in many reported compounds of diverse structures, generally in mononuclear, binuclear, and polynuclear species.[1–5] The d^9 system, on the other hand, plays also a crucial role in several other characterization methods (electronic spectroscopy, magnetic susceptibility and electron paramagnetic resonance) very often connected with the copper(II) chemistry.[6–9] A growing interest in magnetochemistry is noticed in the last decades, especially due to the practical application of the magnetic materials. The magnetically-based methods, *e.g.* EPR and magnetic susceptibility, differ as differences between the magnetic energy levels are crucial for the EPR, while the Boltzmann occupation of all energy levels is analyzed with the magnetic susceptibility. The interaction between the unpaired electrons in a d^9 system can thus be paramagnetic, but ferromagnetic and antiferromagnetic are often discovered as well.[7,10] An absence of the intermetal magnetic interaction (paramagnetism) and its presence (ferromagnetism, antiferromagnetism) is largely related to the coordination geometry of the compounds with a focus on the magnetic path between the adjacent Cu^{II} ions. The distance between the metal centres and more important, the type of bridging of selected ligands enables decisive impact on the magnetic interaction. The bridges are most often monoatomic or triatomic, *e.g.* O–C–O in carboxylates, but other types are found as well.[8,11–13] From the coordination geometry the ground state is also suggested. For the octahedral, square-pyramidal and square-planar, the typical Cu^{II} coordination geometries, the ground state is usually $\{d_{x^2-y^2}\}^1$, with some $\{d_{z^2}\}^1$ exceptions. The structural, as well as the magnetic parameters, are also analyzed in terms of different temperature (300–4 K). A comparable energy range of the

* Author to whom correspondence should be addressed. (E-mail: bojan.kozlevcar@fkkt.uni-lj.si)

experimental temperature and the energy difference between the magnetic states, with thermal motion of the atoms, give important data about the nature of the investigated complexes.

During the last decade, several copper(II) coordination compounds were synthesized in our research group in the frame of the carboxylate and the lignin model (phenol type) families as characteristic ligands. These complexes were analyzed with EPR and magnetic susceptibility methods, given special attention also to the coordination geometry.

Crystal Structure Determination

A crystal structure determination is nowadays one of the most pronounced tools in chemistry, due to its efficiency enabling a determination of the molecular structure from a single crystal. Analyses of the other characterization methods are as a rule connected with the structural data, thus giving stronger and clearer correlation among the complementary characterizing methods. Herein, the molecular structures of the investigated compounds are analyzed in a view of the 'magnetic' unpaired Cu^{II} d^9 electron, a relation to its parent coordination sphere and to more distant adjacent Cu^{II} chromophores with possible magnetic interaction among each other.

Mononuclear compounds reveal the paramagnetic properties, while the binuclear and the polynuclear complexes reveal either the ferromagnetic or the antiferromagnetic interaction between the neighbouring copper(II) centres. A large group of the antiferromagnetically coupled copper(II) ions are the dicopper(II) tetracarboxylates, where four triatomic carboxylates bridge two Cu^{II} ions. The first such structure of copper(II) acetate hydrate $[Cu_2(\mu\text{-}O_2CCH_3)_4(H_2O)_2]$ was described half a century ago, revealing a *paddle-wheel* binuclear moiety.[14]

EPR (ESR)

The electron paramagnetic (spin) resonance measures differences between the magnetic energy levels. They are described by the magnetic quantum numbers m_S and are degenerated in an absence of the magnetic field.[9,15] Due to the applied magnetic field, the energy levels split showing the Zeeman phenomenon.

Two large groups of copper(II) EPR spectra are described, namely for spin S = ½ and S = 1. Spin S = ½ represents the most simple example with two m_S states (–½, +½) and their energy difference (the magnetic resonance condition) is described as energy = $h\nu = g\beta_e B$ (Scheme 1). The symmetry of the magnetic/spin tensor, which often reflects the symmetry of the coordination sphere is the main reason to see one, two or three signals in the spectrum.[16,17] Spin S = ½ is usually characteristic for the mononuclear coordination compounds or polynuclear complexes, where the magnetic interaction between the metal centres is not present (paramagnets).

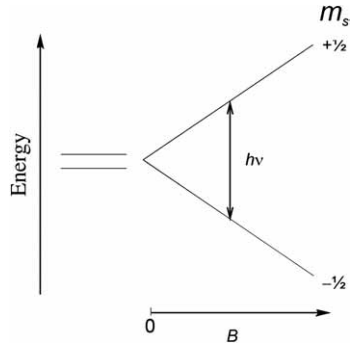

Scheme 1. The Zeeman effect in the EPR experiment for spin S = ½.

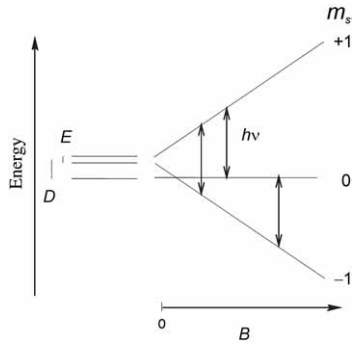

Scheme 2. The Zeeman effect in the EPR experiment for spin S = 1. The magnetic field is parallel with the z axis.

Spin S = 1 is often present in the binuclear complexes, where two spins S = ½ of two adjacent copper(II) ions are coupled *via* a bridging ligand, most often resulting in a ferromagnetic or an antiferromagnetic behaviour. The ferromagnetism is represented by a positive *2J* exchange interaction value (S = 1 triplet ground state, S = 0 singlet first excited state), while the antiferromagnetism by a negative *2J* value (S = 0 singlet ground state, S = 1 triplet first excited state). At the room temperature one can see S = 1 signals (S = 0 is EPR silent – no signals in the EPR spectrum) for the antiferromagnetic species, *e.g.* $[Cu_2(\mu\text{-}O_2CCH_3)_4(H_2O)_2]$ type of complexes.[11,18–20] Usually, there is a ligand bridge between the two Cu^{II} cations, but other types of connection may also take place (*e.g.* π-π interactions, H-bonding). Due to spin S = 1, three magnetic quantum numbers (–1, 0, 1) describe the system, and similarly as for S = ½, the Zeeman effect is noticed in the EPR spectra, splitting the states, almost degenerate at zero magnetic field (Scheme 2).[9,15,19]

Two copper(II) ions for S = 1, theoretically enable 6 EPR signals if no hyperfine splitting is resolved (2 Cu^{II} ions × 3(x, y, z) axes), and each of these signals may be described by an equation, as shown by Wassermann *et al.*[18] (Eqs. (1)–(6)) $B_0 = h\nu/g_e\beta_e$, $D' = D/g_e\beta_e$, $E' = E/g_e\beta_e$, D = the axial zero field splitting parameter, E = the rhombic zero field splitting parameter.

$$B_{x1}^2 = \left(\frac{g_e}{g_x}\right)^2 (B_0 - D' + E')(B_0 + 2E') \quad (1)$$

$$B_{x2}^2 = \left(\frac{g_e}{g_x}\right)^2 (B_0 + D' - E')(B_0 - 2E') \quad (2)$$

$$B_{y1}^2 = \left(\frac{g_e}{g_y}\right)^2 (B_0 - D' - E')(B_0 - 2E') \quad (3)$$

$$B_{y2}^2 = \left(\frac{g_e}{g_y}\right)^2 (B_0 + D' + E')(B_0 + 2E') \quad (4)$$

$$B_{z1}^2 = \left(\frac{g_e}{g_z}\right)^2 \left((B_0 - D')^2 - (E')^2\right) \quad (5)$$

$$B_{z2}^2 = \left(\frac{g_e}{g_z}\right)^2 \left((B_0 + D')^2 - (E')^2\right) \quad (6)$$

Additionally, the Eq. (7) enables the calculation of a type and magnitude of the magnetic interaction.[19]

$$D = -\frac{J}{8}\left(\frac{1}{4}(g_{\parallel} - 2)^2 - (g_{\perp} - 2)^2\right) - \left(g_{\parallel}^2 + \frac{1}{2}g_{\perp}^2\right)\frac{\beta_e^2}{r^3} \quad (7)$$

Magnetic Susceptibility

Magnetic susceptibility (χ) is the degree of the magnetization of a material in response to a magnet. The method measures the Boltzmann occupation of all energy levels. Often the molar magnetic susceptibility χ_M is used for an analysis as a graph of χ_M *versus* T or $\chi_M \cdot T$ *versus* T. A constant $\chi_M \cdot T$ value is characteristic for the paramagnetic species, while the deviation from the constant $\chi_M \cdot T$ to lower values (by decreasing T) reveals an antiferromagnetism (Scheme 3). On the contrary, the deviation to higher values reveals a ferromagnetism. The magnetic susceptibility analysis for the paramagnetic species with a constant $\chi_M \cdot T$ at different temperatures is rarely described in details in the literature. The effective magnetic moment for the paramagnet real samples is above 1.73 μ_B, as expected for the spin contribution ($\mu_{eff} = (n(n+2))^{1/2}$, or $\mu_{eff} = 2(S(S+1))^{1/2}$, n = a number of the unpaired electrons per copper(II) ion, or S = the total spin quantum number). It may be calculated by $\mu_{eff} = 2.828(\chi_M \cdot T)^{1/2}$ (c.g.s. units) from the susceptibility measurements.[10]

The experimental data for some dinuclear compounds can be well reproduced by considering the expression of χ_M:

$$\chi_M = (1-\rho)\frac{2N_A g^2 \beta_e^2}{k_B T(3 + e^{-2J/k_B T})} + \rho\frac{N_A g^2 \beta_e^2}{2k_B T} + \text{TIP} \quad (8)$$

(TIP = temperature independent paramagnetism, ρ = yield of the paramagnetic impurity) derived from the Heisenberg Hamiltonian

$$\hat{H} = -2J\,\hat{S}_1 \cdot \hat{S}_2 \quad (9)$$

for the antiferromagnetic $[Cu_2(\mu\text{-}O_2CCH_3)_4(H_2O)_2]$ introduced by Bleaney and Bowers,).[8,21] Additionally, the expression for the magnetic interaction constant $2J$

$$2J = E_S - E_T = 2k + 4\beta s \quad (10)$$

derived by Kahn, relates its ferro-/antiferro-magnetic character with the spatial symmetry of magnetic orbitals.[8,11] (ferromagnetism – positive $2J$, antiferromagnetism – negative $2J$; k = Coulomb repulsion integral for two centres > 0, s = overlap integral > 0, β = Coulomb one electron integral – orbital energy < 0).

MONONUCLEAR COMPLEXES

The complexes with one copper(II) ion in the coordination sphere were isolated with the bidentate O,O' ligands (carboxylate and methoxyphenol) and with the additional nitrogen or oxygen donor ligand completing the Jahn-Teller distorted octahedron. The two types of the bidentate coordination moieties differ due to the connecting spacer between the two coordinating oxygen atoms, namely, O–C–O and O–C–C–O for the carboxylate and

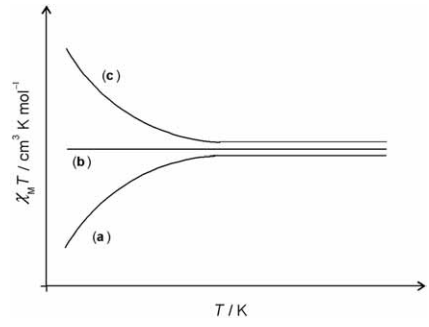

Scheme 3. The magnetic susceptibility graphs $\chi_M \cdot T(T)$ representing antiferromagnetic (a), paramagnetic (b) and ferromagnetic (c) species.

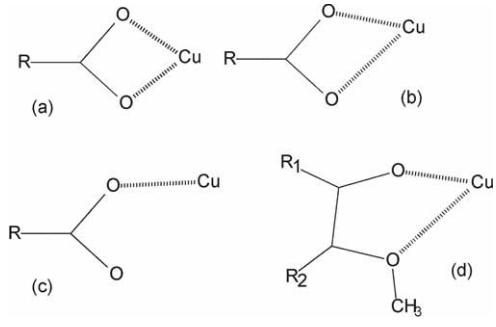

Scheme 4. Coordination modes of the carboxylate ((a) symmetric chelate, (b) asymmetric chelate, and (c) monodentate) and the phenol type of ligands ((d) asymmetric chelate).

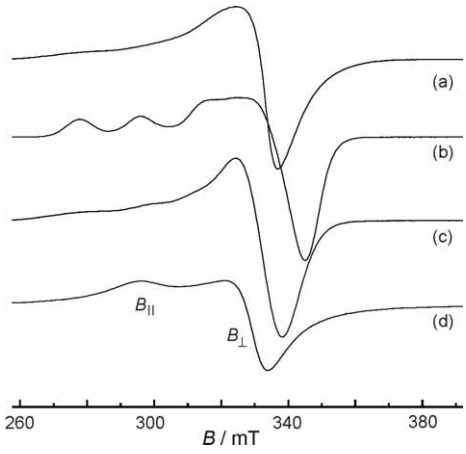

Figure 1. The room *T* axial elongated symmetry spectra of copper(II) salycilates: (a) $[Cu(O_2CC_6H_5O)_2(nia)_2]$ – orthorhombic (nia = nicotinamide); (b) $[Cu(O_2CC_6H_5O)_2(nia)_2]$ – monoclinic; (c) $[Cu(O_2CC_6H_5O)_2(nia)_2(H_2O)_2]$; (d) $[Cu(O_2CC_6H_5O)_2(H_2O)_2] \cdot 2H_2O$). (Reproduced from Ref. 31 with permission of the copyright holders.)

methoxyphenol ligand, respectively. The carboxylate coordination of the herein presented complexes varies from symmetric chelate[22] to asymmetric chelate,[23–27] and finally to monodentate[28,29] (Scheme 4). Among these, the salycilates show several isomers.[23,29–31] Three isomers were isolated also with a ligand vanillin (methoxyphenol) all showing the asymmetric chelate coordination (Scheme 4d).[32–34] The molecular structures of the mentioned mononuclear carboxylate complexes do not change significantly by decreasing the temperature, however a structural change is noticed in the *cis* isomer of the vanillin complex *cis*-$[Cu(O_2C_8H_7O)_2(H_2O)_2]$ with the variation of the temperature.[33,34]

Among several types of the EPR spectra known for the mononuclear (paramagnetic) Cu^{II} species with S = ½, those with two signals $g_{\perp(x,y)} < g_{||(z)}$ ($B_{\perp(x,y)} > B_{||(z)}$), representing elongated axial symmetry of the magnetic/spin tensor, which is often related to the symmetry of the coordination sphere but not necessarily identical (Figure 1d), are the most often (one coordination axis (*z*) is significantly longer than the other two (*x*, *y*) (Scheme 5a). The $B_{||}$ signal may be hyperfine split to four signals due to the Cu^{II} unpaired electron (S = ½) interaction with Cu^{II} nucleus spin (I = 3/2). The hyperfine splitting is clearly visible in the Figure 1b with two of the $B_{||}$ signals below 300 mT, and the other two overlapped with the $B_{\perp}$ signal.

The next group of the S = ½ system EPR spectra are those with only one signal at 320 mT (Figure 2a), revealing the isotropic symmetry ($g_1 = g_2 = g_3 = g$, $B_1 = B_2 = B_3$) or similar coordination bond distances for all six Cu–L of the octahedron (Scheme 5d) or five Cu–L in the square-pyramid. This type of coordination is noticed for the square-pyramid CuO_3NO chromophore in a polynuclear $[Cu(\mu\text{-}O_2CH)_2(3\text{-pyOH})]_n$, 3-pyOH = 3-hydroxypyridine (Cu–O,N(equatorial) 1.945-2.016 Å, Cu–O(axial) 2.247 Å).[35] The polynuclear complexes often show S = ½ EPR signals in the range 298–100 K (Figure 2) due to inappropriate coordination *via* non-magnetic $\{d_{z^2}\}^2$ Cu orbital, giving a very weak or no exchange interaction.

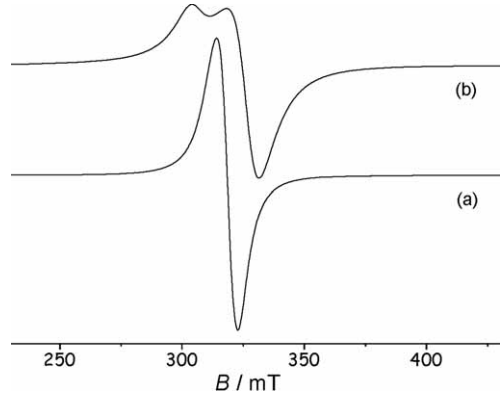

Figure 2. Pseudo isotropic and axial symmetry S = ½ EPR spectra of the polynuclear complexes $[Cu(\mu\text{-}O_2CH)_2(3\text{-pyOH})]_n$ (3-pyOH = 3-hydroxypyridine) (a) and $[Cu_2(\mu\text{-}O_2CH)_2(\mu\text{-}3\text{-pyOH})_2(3\text{-pyOH})_2(O_2CH)_2]_n$ (b) (100 K), respectively.[35]

The third type of the S = ½ spectra shows three signals $B_{x(1)}$, $B_{y(2)}$ and $B_{z(3)}$ revealing the rhombic symmetry of the coordination sphere (Figure 3, Figure 5, 115 K). These signals correspond to the three different main axes *x*, *y* and *z*, of the magnetic tensor, all of different length (Scheme 5c). When two of these three signals are very

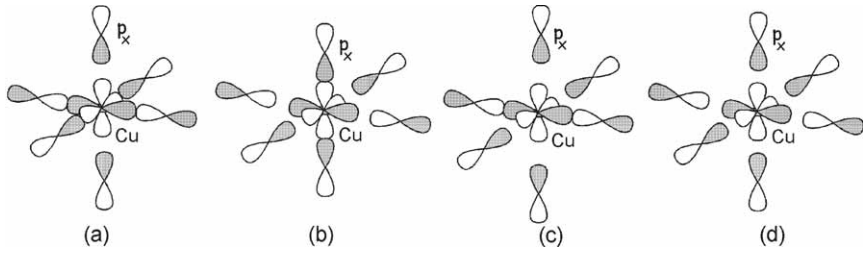

Scheme 5. The coordination bond orbital arrangement showing different types of the octahedral copper(II) coordination sphere: (a) axial elongated, (b) axial compressed, (c) rhombic, and (d) isotropic. The distance between the ligand p_x orbital and the copper(II) d_{x2-y2} or d_{z2} orbital is suggesting the length of the coordination bond.

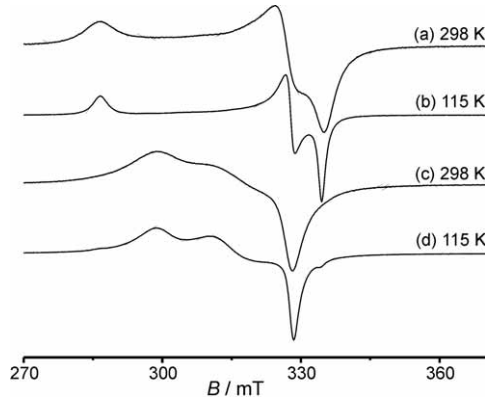

Figure 3. The rhombic symmetry EPR spectra of vanillin compounds *trans*-[$Cu(O_2C_8H_7O)_2(H_2O)_2$] (a, b) and *trans*-[$Cu(O_2C_8H_7O)_2(H_2O)_2$] · $2H_2O$ (c, d). (Reproduced from Ref. 34 with permission of the copyright holders.)

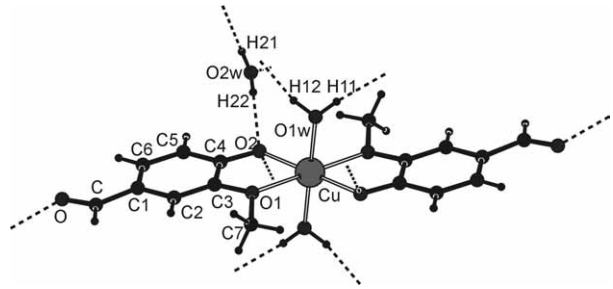

Figure 4. The molecular structure of a vanillin complex *trans*-[$Cu(O_2C_8H_7O)_2(H_2O)_2$] · $2H_2O$. (Reproduced from Ref. 34 with permission of the copyright holders.)

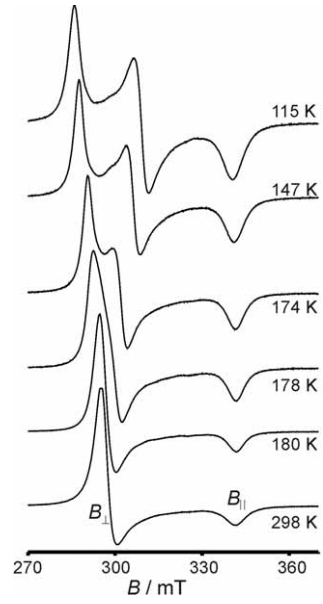

Figure 5. A temperature dependence of the EPR spectra of a vanillin compound *cis*-[$Cu(O_2C_8H_7O)_2(H_2O)_2$]. (Reproduced from Ref. 33 with permission of the copyright holders.)

close to each other, the spectrum is than similar to the axial elongated type of spectrum (Figures 1, 3, 5). Although the spectrum of the vanillin complex *trans*-[$Cu(O_2C_8H_7O)_2(H_2O)_2$] · $2H_2O$ shows three signals (Figure 3c, d), two of three coordination bonds are almost of same length (Cu–O(H_2O) 1.994 Å, Cu–O(hydroxy) 1.950 Å), while the third is longer (Cu–O(methoxy) 2.334 Å). The rhombic EPR differentiation may be explained by different ligands in the two similarly long coordination axes (H_2O)O–Cu–O(H_2O) and (hydroxy)O–Cu–O(hydroxy), respectively (Figure 4).[34]

The least commonly found EPR spectra of $S = ½$ are of compressed axial type $g_{\perp(x,y)} > g_{\|(z)}$ ($B_{\perp(x,y)} < B_{\|(z)}$), representing compressed axial symmetry of the coordination sphere (one coordination axis (z) is significantly shorter than the other two (x, y), Scheme 5b, Figure 5, 298 K). So far we succeeded to obtain only one such example, namely the spectrum of the complex *cis*-[$Cu(O_2C_8H_7O)_2(H_2O)_2$]. Spectra for this compound differ with the temperature when recorded, from the signals representing the compressed axial symmetry at room *T*, to the signals due to the rhombic symmetry at 115 K (Figure 5). The molecular structures from the data obtained at 293 K and at 115 K agree with the EPR observations.[33,34] Herein, two (H_2O)O–Cu–O(methoxy) coordination axes change from two equal length axes (2.087 + 2.260 Å) found at room *T* to two different length axes (2.020 + 2.151 Å, 2.163 + 2.354 Å) noticed at 115 K. The (hydroxy)O–Cu–O(hydroxy) axis remain almost the same (Scheme 6). This phenomenon was ana-

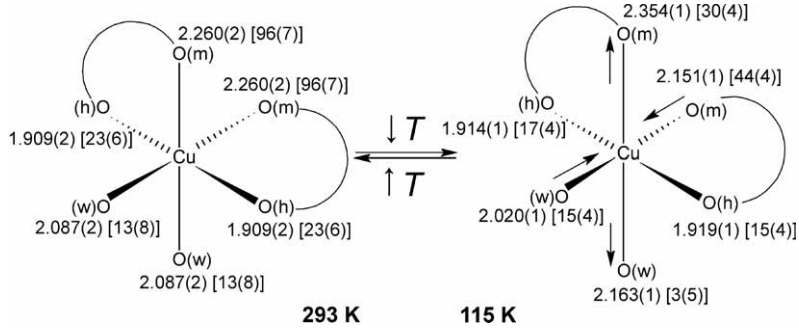

Scheme 6. A temperature induced reversible change of the Cu–O coordination bond distances (Å) in *cis*-[$Cu(O_2C_8H_7O)_2(H_2O)_2$] (h – hydroxy, m – methoxy, w – water). Thermal motion analysis (TMA, MSDA): Cu–O $<d^2>$ values (x 10^4 $Å^2$) are in square brackets. (Reproduced from Ref. 33 with permission of the copyright holders.)

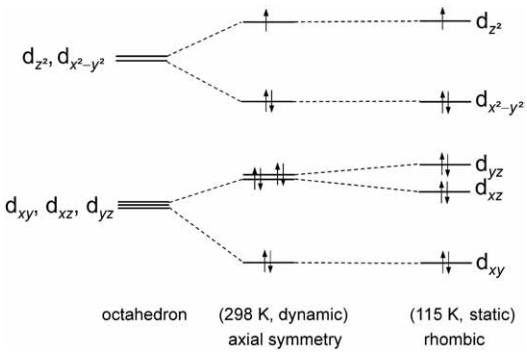

Scheme 7. The orbital splitting diagram of a Jahn-Teller compressed octahedron along the *z* axis. (Reproduced from Ref. 33 with permission of the copyright holders.)

lyzed by a thermal motion analysis – TMA (see also mean square displacement amplitude – MSDA), a method incorporated also in PLATON,[36,37] and explained by a pseudo Jahn-Teller[38–40] distortion (Scheme 7). The librational dynamic disorder of the Jahn-Teller distorted axes is leading to an equalization of the determined bond lengths, imitating a higher symmetry in the structure at higher temperatures. The $\{d_{z^2}\}^1$ ground state is assigned to this compound, while the $\{d_{x2-y2}\}^1$ to all the other herein described complexes.

DINUCLEAR COMPLEXES

The complexes with two copper(II) ions in the coordination sphere are mostly found as isolated dicopper(II) tetracarboxylates with triatomic O–C–O bridges of *paddle-wheel* type (Scheme 8a),[24,25,41–47] and some other examples[48,49] as pyridone *paddle-wheel* complexes (triatomic N–C–O bridges). The complexes with polynuclear structures of binuclear building blocks are described in the next section.

The EPR spectra of the isolated dicopper(II) tetracarboxylate complexes (Figure 6a, b) show three signals

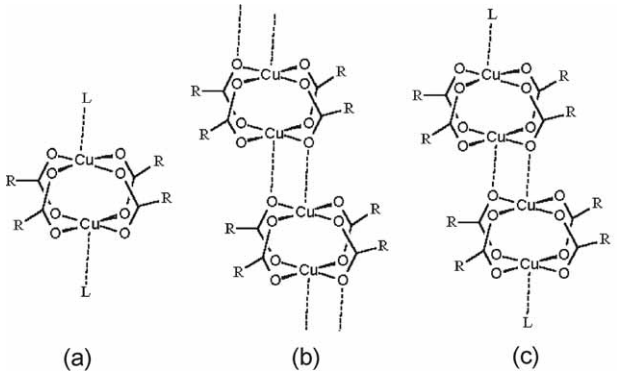

Scheme 8. Various structural types in dicopper(II) tetracarboxylates by dimeric building blocks and terminal ligand L: (a) isolated dinuclear; (b) polynuclear; (c) tetranuclear. (Reproduced from Ref. 45 with permission of the copyright holders.)

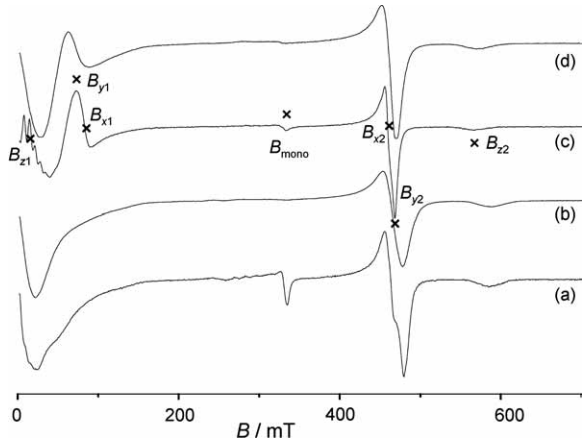

Figure 6. The EPR $S = 1$ triplet signals of vanillic acid compounds $[Cu_2(\mu\text{-}O_2CC_7H_7O_2)_4(H_2O)_2]$ ((c) 116 K; (d) 298 K) and mixed carboxylato $[Cu_2(\mu\text{-}O_2CC_7H_7O_2)_2(\mu\text{-}O_2CCH_3)_2]$ (= after removal of $[Cu_2(\mu\text{-}O_2CC_7H_7O_2)_2(\mu\text{-}O_2CCH_3)_2(CH_3OH)_2]$ from the mother liquid) ((a) 116 K; (b) 298 K). (Reproduced from Ref. 46 with permission of the copyright holders.)

(B_{z1}, $B_{\perp 2(x2,\ y2)}$, B_{z2},) which are typical for the antiferromagnetically coupled copper(II) centers with spin $S = 1$ in the range 0–700 mT for the X-band frequency region. Such a spectrum is usually represented as a $[Cu_2(\mu\text{-}O_2CCH_3)_4(H_2O)_2]$ type,[14,19,50] due to the first reported structure of this kind. Theoretically, six signals would be expected (B_{x1}, B_{x2}, B_{y1}, B_{y2}, B_{z1}, B_{z2}, Eqs. (1)–(6)),[18] but due to a large axial zero field splitting parameter D ($> h\nu \sim 0.32$ cm^{-1} for an X-band spectrum), B_{x1} and B_{y1} ($B_{\perp 1}$) are as a rule not observed for this type of complexes. However, for the vanillic acid complex $[Cu_2(\mu\text{-}O_2CC_7H_7O_2)_4(H_2O)_2]$[46,50,51] with D (= 0.30 cm^{-1}) $< h\nu$ (= 0.32 cm^{-1}), all six $S = 1$ signals are observed (Figure 6c, d) in the X-band spectra. The calculated antiferromagnetic intrabinuclear magnetic interaction *2J* for the dicopper(II) tetracarboxylates can be calculated *via* the 'Wasserman' Eqs. (1)–(7)[18,19] and its magnitude is usually in the range around –300 cm^{-1}.

If almost fleeting description of the susceptibility data are available for the $S = ½$ species (*e.g.* mononuclear), the complexes with two or more copper(II) ions are regularly described with a molar magnetic susceptibility χ_M analysis. The EPR and the magnetic susceptibility data usually agree with a large antiferromagnetic exchange interaction *2J*. Complexes with a strong antiferromagnetism show a lower μ_{eff} (= $2.828(\chi_M \cdot T)^{1/2}$) value than 1.73 μ_B (the spin only value for one uncoupled electron) already at room temperature, followed by a significant decrease of the χ_M or $\chi_M \cdot T$ value by decreasing temperature (Figure 7). An increase of χ_M below 60 K can be attributed to the 'paramagnetic impurities'.

The antiferromagnetism of dicopper(II) tetracarboxylates can be described by an orbital overlap of the bridging ligand (*syn*, *syn* orientation in this case) and both metal ions. The superexchange mechanism through a li-

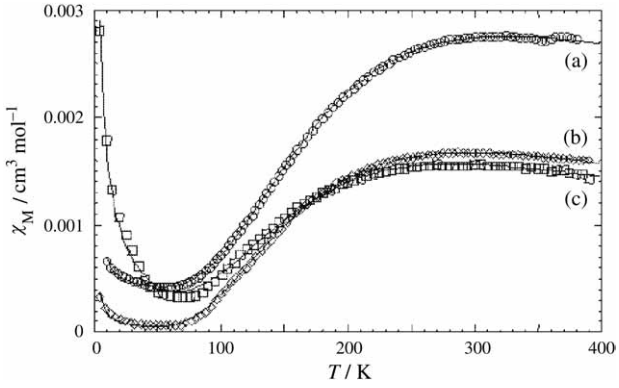

Figure 7. The experimental susceptibility data for the hexanoate compounds $[\{Cu_2(\mu\text{-}O_2CC_5H_{11})_4(urea)\}_2]$ (a), $[Cu_2(\mu\text{-}O_2CC_5H_{11})_4(urea)_2]$ (b); and $[Cu_2(\mu\text{-}O_2CC_5H_{11})_4]_n$ (c), respectively, with the appropriate theoretical data (full lines, Eqs. (8) and (9). (Reproduced from Ref. 45 with permission of the copyright holders.)

gand bridge is now a preferred way of describing the antiferromagnetic exchange pathway. The equatorially coordinated oxygen atoms (Cu–O(eq) 1.94–1.99 Å) in the square-planar coordination sphere CuO_4N or CuO_4O are closer than the axial atom (Cu–O,N(ax) 2.07–2.24 Å),[53] thus the equatorially oriented Cu orbital $\{d_{x2-y2}\}^1$ is the magnetic, while the axially $\{d_{z2}\}^2$ is not. Theoretically, the overlap of the 'magnetic' Cu orbital (with one electron) on both sides of the exchange pathway (Cu–L–Cu) plays a crucial role in determining the ferromagnetic or the antiferromagnetic nature of the exchange interaction. A strong bonding (orbital overlap) of the magnetic orbitals usually leads to the antiferomagnetic interaction, while non-bonding (= a bonding with the non-magnetic orbitals; or orthogonality of the magnetic orbitals) might lead to the ferromagnetism. From the quantum mechanics it is shown as a competition among both options ($J = J_{AF} + J_F$).[20,54] Since the antiferromagnetic interaction is essentially of a higher magnitude[55] (a few 100 cm^{-1}), the weaker ferromagnetism (up to a few 10 cm^{-1}) is possible only without a direct bonding of the Cu magnetic orbital

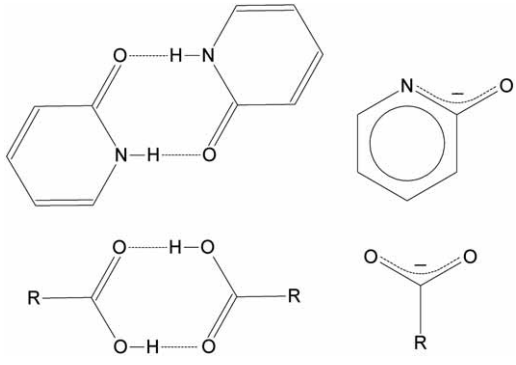

Scheme 9. An analogy between 2-pyridone and carboxylic acid and their anions. (Reproduced from Ref. 49 with permission of the copyright holders.)

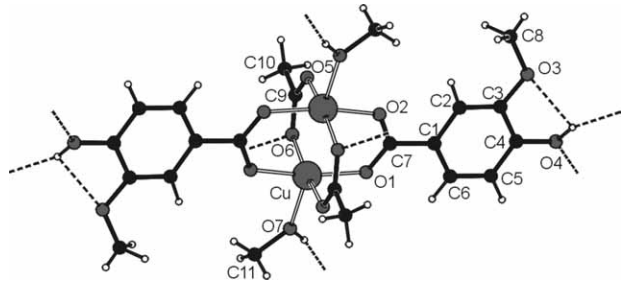

Figure 8. Two types of the bridging carboxylate ligands in a binuclear copper(II) tetracarboxylate complex $[Cu_2(\mu\text{-}O_2CC_7H_7O_2)_2(\mu\text{-}O_2CCH_3)_2(CH_3OH)_2]$. (Reproduced from Ref. 46 with permission of the copyright holders.)

to the ligand on both sides of a bridge. The length of the coordination bond is the basic parameter determining occupancy (one or two electrons) of the metal d orbital oriented toward the ligand.

2-Pyridone (= HL) complexes $[Cu_2(\mu\text{-}L)_4(HL)_2]$ and $[Cu_2(\mu\text{-}O_2CH)_2(\mu\text{-}L)_2(HL)_2]\cdot 2CH_3CN$[48] show a strong analogy to related *paddle-wheel* dicopper(II) tetracarboxylate complexes, namely with four N–C–O and O–C–O bridges, respectively (Scheme 9). Due to six EPR $S = 1$ signals found for $[Cu_2(\mu\text{-}L)_4(HL)_2]$ and related N–C–O or N–C–N bridged *paddle-wheel* complexes,[55–57] while all six signals so rarely found in numerous dicopper(II) tetracarboxylates,[45] an important role of the bridge type for an appearance or an absence of the $B_{\perp 1(x1,\,y1)}$, is suggested. The *paddle-wheel* nature of 2-pyridone complexes is observed also in the $\chi_M{\cdot}T(T)$ graphs, revealing strong antiferromagnetism (~ –330 cm^{-1}).

The complexes with two different bridges in the *paddle-wheel* $[Cu_2(\mu\text{-}O_2CH)_2(\mu\text{-}L)_2(HL)_2]$ (= after removal of $[Cu_2(\mu\text{-}O_2CH)_2(\mu\text{-}L)_2(HL)_2]\cdot 2CH_3CN$ from the mother liquid) and $[Cu_2(\mu\text{-}O_2CC_7H_7O_2)_2(\mu\text{-}O_2CCH_3)_2]$ (= after removal of $[Cu_2(\mu\text{-}O_2CC_7H_7O_2)_2(\mu\text{-}O_2CCH_3)_2(CH_3OH)_2]$ (Figure 8) from the mother liquid) are giving related $S = 1$ EPR and χ_M results as regular copper(II) acetate type (B_{z1}, $B_{\perp 2(x2,\,y2)}$, B_{z2},). EPR and susceptibility measurements were performed by the dry solid samples! These data suggest that different bridges of different ligands may serve for the same type of antiferromagnetic interaction in the *paddle-wheel* complex, if only they have similar geometry. Interestingly, we managed to find the complexes with all six $S = 1$ EPR signals just and only for the complexes $[Cu_2(\mu\text{-}L)_4(HL)_2]$ and $[Cu_2(\mu\text{-}O_2CC_7H_7O_2)_4(H_2O)_2]$ that are the closest analogues of the mentioned mixed *paddle-wheel* complexes.

POLYNUCLEAR COMPLEXES

Only one typical polynuclear complex (from monomeric building blocks), $[Cu(\mu\text{-}O_2CH)_2(3\text{-}pyOH)]_n$, 3-pyOH = 3-hydroxypyridine, is shown herein (Figure 9). The EPR

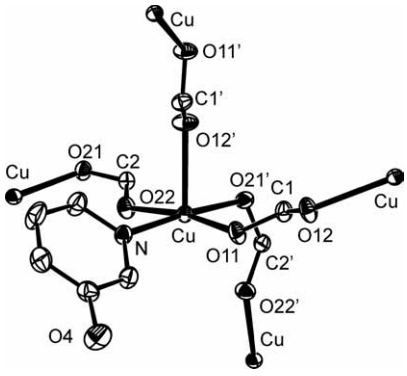

Figure 9. Two types of methanoate bridges among the Cu–3-pyOH moieties in a polymeric structure of $[Cu(\mu\text{-}O_2CH)_2(3\text{-pyOH})]_n$. (Cu···Cu: *syn-anti* 4.690 Å, *anti-anti* Cu···Cu 5.935 Å). All H-atoms are omitted for clarity. (Reproduced from Ref. 35 with permission of the copyright holders.)

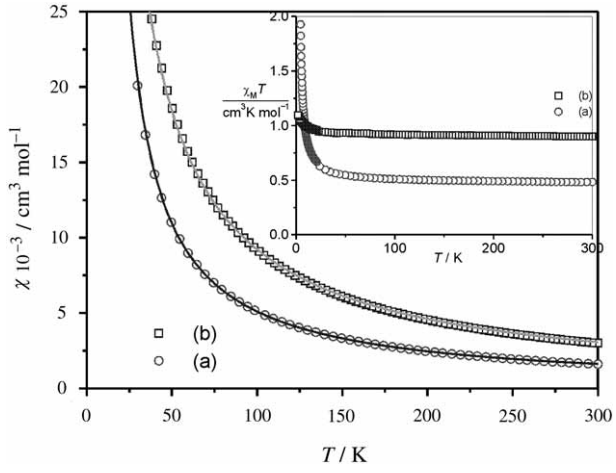

Figure 10. The magnetic properties χ_M and $\chi_M \cdot T$ (inset) of the 3-hydroxypyridine complexes $[Cu(\mu\text{-}O_2CH)_2(3\text{-pyOH})]_n$ (a); and $[Cu_2(\mu\text{-}O_2CH)_2(\mu\text{-}3\text{-pyOH})_2(3\text{-pyOH})_2(O_2CH)_2]_n$ (b). The full lines in the graph χ_M correspond to the Curie-Weiss law. (Reproduced from Ref. 35 with permission of the copyright holders.)

spectra for this complex were recorded at 298 and 100 K, and a pseudo isotropic signal of $S = ½$ is observed (Figure 2a). This signal originates from similar coordination bond distances Cu–O,N(eq) and Cu–O(ax), 1.945–2.016 Å and 2.247 Å, respectively. The susceptibility measurements were performed in the range 4 K – room *T* and a weak ferromagnetism was observed below 50 K (an inset in Figure 10). This is in the agreement with the EPR data in the range 100 K – room *T*, where these measurements were recorded. The magnetic interaction takes place *via* the *syn-anti* coordinated ligands (O21–C2–O22), due to the magnetic $\{d_{x^2-y^2}\}^1$ Cu bonding orbitals on both sides of the bridge (this is not the case for the *anti-anti* O11–C1–O12 bridge; see Figure 9). This seems to be the main reason concerning the magnetic interaction, and not a Cu···Cu distance. The ferromagnetism found for this compound is related to a non-planarity of a bridging network, that significantly reduces especially the antiferromagnetic part of the interaction to the extent, enabling the ferromagnetic part to be predominant ($J = J_{AF} + J_F$).

A vast majority of the polynuclear compounds are those composed of binuclear units and are of three types. A complex $[Cu_2(\mu\text{-}O_2CCH_3)_4(\mu\text{-nia})]_n$, nia = nicotinamide,[41] is formed of *paddle-wheel* dicopper(II) tetraacetate building blocks, with the axial nicotinamide serving as a bridging ligand, coordinated *via* pyridine N atom (Cu–N 2.158 Å) and amide O atom (Cu–O 2.146 Å) (Figure 11). It is a rare example of nia acting as bidentate ligand.[59–61] The EPR spectra (room *T*, 150 K) are typical for the $[Cu_2(\mu\text{-}O_2CCH_3)_4(H_2O)_2]$ type, supporting intra-binuclear antiferromagnetic interaction and no or negligible inter-binuclear interactions. A rare analogous structure is reported for $[Cu_2(\mu\text{-}O_2CCH_3)_4(\mu\text{-dena})]_n$, dena = *N*,*N*-diethylnicotinamide.[62]

The second type is a chain of binuclear *paddle-wheel* units, without an additional spacer between them. A partial description of these complexes is reported in the lit-

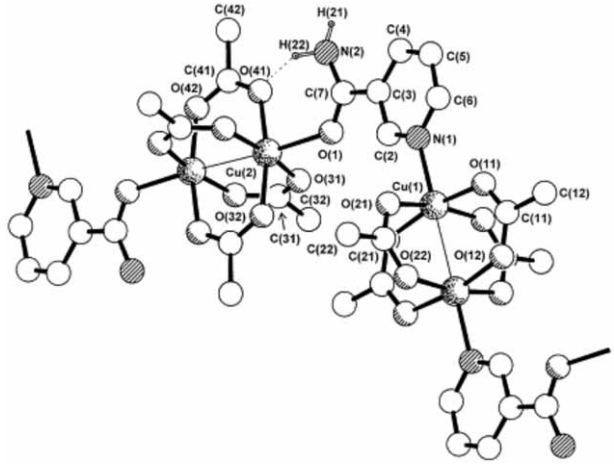

Figure 11. A representation of the polymeric compound $[Cu_2(\mu\text{-}O_2CCH_3)_4(\mu\text{-nia})]_n$, nia = nicotinamide. (Reproduced from Ref. 41 with permission of the copyright holders.)

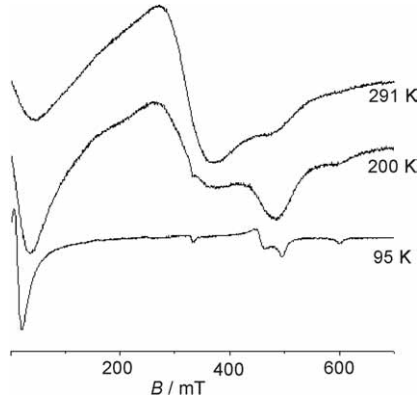

Figure 12. EPR spectra of the polymeric compound $[Cu_2(\mu\text{-}O_2CC_5H_{11})_4]_n$, measured at different temperatures. (Reproduced from Ref. 45 with permission of the copyright holders.)

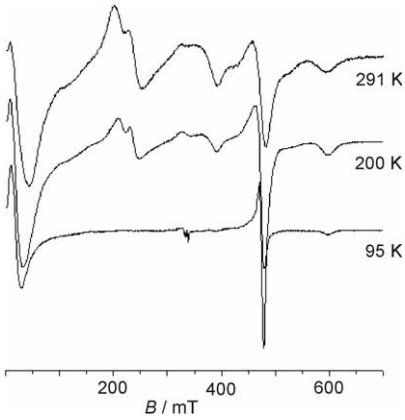

Figure 13. EPR spectra of the tetranuclear compound $[\{Cu_2(\mu\text{-}O_2CC_5H_{11})_4(urea)\}_2]$, measured at different temperatures. (Reproduced from Ref. 45 with permission of the copyright holders.)

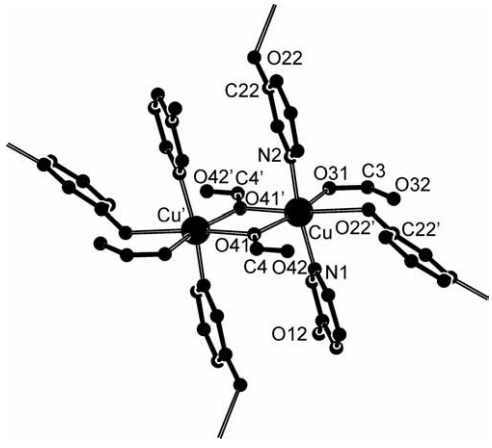

Figure 14. The dinuclear unit in a structure of $[Cu_2(\mu\text{-}O_2CH)_2(\mu\text{-}3\text{-}pyOH)_2(3\text{-}pyOH)_2(O_2CH)_2]_n$, forming a 2-D network. All H-atoms are omitted for clarity. (Reproduced from Ref. 35 with permission of the copyright holders.)

erature,[63–66] and we prepared a detailed EPR and a susceptibility analysis of related families,[45] *e. g.* ($[Cu_2(\mu\text{-}O_2CC_5H_{11})_4(urea)_2]$,[43,67] $[\{Cu_2(\mu\text{-}O_2CC_5H_{11})_4(urea)\}_2]$ and $[Cu_2(\mu\text{-}O_2CC_5H_{11})_4]_n$[43] (Scheme 8). The $[Cu_2(\mu\text{-}O_2CC_5H_{11})_4]_n$ EPR spectra show the triplet signals for $S = 1$ of the intra-binuclear interaction (copper(II) acetate hydrate type), though not when recorded at the room T (Figure 12). At this temperature some broad signals prevail over $S = 1$ triplet signals, but they gradually disappear by decreasing the temperature, while simultaneously the triplet signals appear. The replacement is complete at 100 K.

It is suggested that the high temperature broad signals are most likely related to the $S = 1$ inter-binuclear interactions, meaning among $S = 1$ of the adjacent dinuclear building blocks.[68–70] Similar EPR spectra, a combination of high T broad signals and low T triplet $S = 1$ signals (Figure 13) were reported for $[\{Cu_2(\mu\text{-}O_2CC_5H_{11})_4(urea)\}_2]$, that is a hybrid type of the isolated binuclear $[Cu_2(\mu\text{-}O_2CC_5H_{11})_4(urea)_2]$ and a polynuclear $[Cu_2(\mu\text{-}O_2CC_5H_{11})_4]_n$, (Scheme 8). The susceptibility measurements were performed for each case of these three groups ($[Cu_2(\mu\text{-}O_2CC_5H_{11})_4(urea)_2]$, $[\{Cu_2(\mu\text{-}O_2CC_5H_{11})_4(urea)\}_2]$ and $[Cu_2(\mu\text{-}O_2CC_5H_{11})_4]_n$ (Figure 7). All possible intra-binuclear and inter-binuclear magnetic interactions were taken into account, but an antiferromagnetic interaction inside the binuclear units is the only one that seems to be important in all three compounds. There may also be a ferromagnetic interaction among the binuclear units in a polymeric and a hybrid complex, but it is at least a magnitude weaker than the intra-binuclear antiferromagnetism, and thus it is difficult to confirm its presence. The fact that the axial coordination in these *paddle-wheel* complexes is serving as a basis for the inter-binuclear connection, and the lengths of the coordination bonds are Cu–O(eq) < Cu–O(ax), a significant magnetic interaction in the axial direction may not be expected.

The last presenting type of the polynuclear structures with binuclear building blocks is $[Cu_2(\mu\text{-}O_2CH)_2(\mu\text{-}3\text{-}pyOH)_2(3\text{-}pyOH)_2(O_2CH)_2]_n$, 3-pyOH = 3-hydroxypyridine.[35] Herein, two 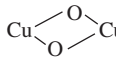 monoatomic methanoato oxygen atoms bridge two Cu^{II} ions, while two 3-hydroxypyridine molecules are *N*-coordinated to each Cu ion perpendicular to the central double bridge moiety (Figure 14). Similar coordination moieties are rarely described.[71] The axial positions of the binuclear units are fulfilled by O22' from 3-pyOH of the adjacent dimer. The EPR spectra at room T and 116 K show two $S = ½$ elongated axial symmetry signals (Figure 2b), while the susceptibility measurements reveal almost negligible ferromagnetic interaction below 30 K (an inset in Figure 10). A very weak magnetic interaction is in accordance with the $Cu(d_{x^2-y^2})^1$–L(ligand)–$Cu(d_{z^2})^2$ intra- and inter-binuclear bridging coordination bonds (Cu–O41–Cu', 1.986 and 2.415 Å, Cu–N2(3-pyOH)O22–Cu', 2.002 and 2.732 Å), respectively.

CONCLUSIONS

The copper(II) complexes presented in this work are of all three general groups, namely, mononuclear, binuclear and polynuclear. The analysis of the EPR spectra and the magnetic susceptibility data reveal a clear correlation with the structures of the analyzed complexes and/or their basic building blocks. The longer and shorter coordination bonds, described by the Jahn-Teller theorem clearly play the crucial role in the exchange interactions in these copper(II) coordination compounds.

Acknowledgement. – We thank Prof. Peter Strauch (Univ. Potsdam, Germany) for helpful discussions. The financial support of the Ministry of Higher Education, Science and Technology, Republic of Slovenia, through grants P1-0175 and X-2000, is gratefully acknowledged.

REFERENCES

1. M. Melnik, M. Kabešova, M. Koman, L. Macaškova, and C. E. Holloway, *J. Coord. Chem.* **50** (2000) 177–322.
2. M. Melnik, M. Kabešova, M. Koman, L. Macaškova, and C. E. Holloway, *J. Coord. Chem.* **48** (1999) 271–374.
3. M. Melnik, M. Kabešova, M. Koman, L. Macaškova, J. Garaj, C. E. Holloway, and A. Valent, *J. Coord. Chem.* **45** (1998) 147–359.
4. M. Melnik, M. Kabešova, L. Macaškova, and C. E. Holloway, *J. Coord. Chem.* **45** (1998) 31–145.
5. M. Melnik, M. Kabešova, M. Dunaj Jurčo, and C. E. Holloway, *J. Coord. Chem.* **41** (1997) 35–182.
6. A. B. P. Lever, *Inorganic Electronic Spectroscopy*, Elsevier, 1984.
7. R. L. Dutta and A. Syamal, *Elements of Magnetochemistry*, Affiliated East-West PVT Ltd, 1993.
8. O. Kahn, *Molecular Magnetism*, VCH, New York, 1993.
9. F. E. Mabbs and D. Collison, *Electron Paramagnetic Resonance of d Transition Comounds*, Vol. 16, Elsevier, Amsterdam, 1992.
10. J. D. Lee, *Concise Inorganic Chemistry*, Chapman & Hall, London, 1996, pp. 653–678.
11. M. Verdaguer, *Polyhedron* **20** (2001) 1115–1128.
12. P. J. Hay, J. C. Thibeault, and R. Hoffmann, *J. Am. Chem. Soc.* **97** (1975) 4884–4899.
13. S. Mishra, S. Daniele, and L. G. Hubert-Pfalzgraf, *Chem. Soc. Rev.* **36** (2007) 1770–1787.
14. J. N. van Niekerk, and F. R. L. Schoening, *Acta Cryst.* **6** (1953) 227–232.
15. A. Bencini and D. Gatteschi, in *Inorganic Electronic Structure and Spectroscopy*, Vol. 1, Wiley-Interscience, 1999, pp. 93–159.
16. B. J. Hathaway and D. E. Billing, *Coord. Chem. Rev.* **5** (1970) 143–207.
17. E. Garribba and G. Micera, *J. Chem. Educ.* **83** (2006) 1229–1232.
18. E. Wasserman, L. C. Snyder, and W. A. Yager, *J. Chem. Phys.* **41** (1964) 1763–1772.
19. T. D. Smith and J. R. Pilbrow, *Coord. Chem. Rev.* **13** (1974) 173–278.
20. M. Julve, M. Verdaguer, A. Gleizes, M. Philoche Levisalles, and O. Kahn, *Inorg. Chem.* **23** (1984) 3808–3818.
21. B. Bleaney and K. D. Bowers, *Proc. Roy. Soc. London, A* **214** (1952) 451–465.
22. I. Leban, P. Šegedin, and K. Gruber, *Acta Crystallogr. C* **52** (1996) 1096–1098.
23. I. Leban, B. Kozlevčar, J. Sieler, and P. Šegedin, *Acta Crystallogr. C* **53** (1997) 1420–1422.
24. B. Kozlevčar, N. Lah, D. Žlindra, I. Leban, and P. Šegedin, *Acta Chim. Slov.* **48** (2001) 363–374.
25. B. Kozlevčar, A. Murn, K. Podlipnik, N. Lah, I. Leban, and P. Šegedin, *Croat. Chem. Acta* **77** (2004) 613–618.
26. M. Petrič, I. Leban, and P. Šegedin, *Polyhedron* **15** (1996) 4277–4282.
27. N. Lah, L. Golič, P. Šegedin, and I. Leban, *Acta Crystallogr. C* **55** (1999) 1056–1058.
28. M. Petrič, F. Pohleven, I. Turel, P. Šegedin, A. J. P. White, and D. J. Williams, *Polyhedron* **17** (1998) 255–260.
29. N. Petrovčič, B. Kozlevčar, L. Golič, I. Leban, and P. Šegedin, *Acta Crystallogr. C* **55** (1999) 176–178.
30. N. N. Hoang, F. Valach, and M. Melnik, *Z. Kristall.* **208** (1993) 27–33.
31. B. Kozlevčar, S. Fajfar, M. Petrič, F. Pohleven, and P. Šegedin, *Acta Chim. Slov.* **43** (1996) 385–395.
32. B. Kozlevčar, B. Mušič, N. Lah, I. Leban, and P. Šegedin, *Acta Chim. Slov.* **52** (2005) 40–43.
33. B. Kozlevčar, A. Golobič, and P. Strauch, *Polyhedron* **25** (2006) 2824–2828.
34. B. Kozlevčar, M. B. Humar, P. Strauch, and I. Leban, *Z. Naturforsch. B* **60** (2005) 1273–1277.
35. B. Kozlevčar, L. Glažar, G. Pirc, Z. Jagličić, A. Golobič, and P. Šegedin, *Polyhedron* **26** (2007) 11–16.
36. A. L. Spek, *J. Appl. Crystallogr.* **36** (2003) 7–13.
37. L. J. Farrugia, *J. Appl. Cryst.* **30** (1997) 565.
38. M. A. Halcrow, *J. Chem. Soc., Dalton Trans.* (2003) 4375–4384.
39. L. R. Falvello, *J. Chem. Soc., Dalton Trans.* (1997) 4463–4475.
40. K. Prout, A. Edwards, V. Mtetwa, J. Murray, J. F. Saunders, and F. J. C. Rossotti, *Inorg. Chem.* **36** (1997) 2820–2825.
41. B. Kozlevčar, I. Leban, I. Turel, P. Šegedin, M. Petrič, F. Pohleven, A. J. P. White, D. J. Williams, and J. Sieler, *Polyhedron* **18** (1999) 755–762.
42. B. Kozlevčar, N. Lah, I. Leban, I. Turel, P. Šegedin, M. Petrič, F. Pohleven, A. J. P. White, D. J. Williams, and G. Giester, *Croat. Chem. Acta* **72** (1999) 427–441.
43. B. Kozlevčar, N. Lah, S. Makuc, P. Šegedin, and F. Pohleven, *Acta Chim. Slov.* **47** (2000) 421–433.
44. B. Kozlevčar, N. Lah, I. Leban, F. Pohleven, and P. Šegedin, *Croat. Chem. Acta* **73** (2000) 733–741.
45. B. Kozlevčar, I. Leban, M. Petrič, S. Petriček, O. Roubeau, J. Reedijk, and P. Segedin, *Inorg. Chim. Acta* **357** (2004) 4220–4230.
46. B. Kozlevčar, D. Odlazek, A. Golobič, A. Pevec, P. Strauch, and P. Šegedin, *Polyhedron* **25** (2006) 1161–1166.
47. N. Lah, G. Giester, P. Šegedin, A. Murn, K. Podlipnik, and I. Leban, *Acta Crystallogr. C* **57** (2001) 546–548.
48. L. Glažar, M. Radišek, P. Šegedin, and A. Golobič, *Acta Crystallogr. C* **61** (2005) M526–M528.
49. B. Kozlevčar, M. Radišek, Z. Jagličić, F. Merzel, L. Glažar, A. Golobič, and P. Šegedin, *Polyhedron* **26** (2007) 5414–5419.
50. R. C. Mehrotra and R. Bohra, *Metal Carboxylates*, Academic Press, London, 1983.
51. T. Glowiak, H. Kozlowski, L. S. Erre, B. Gulinati, G. Micera, A. Pozzi, and S. Bruni, *J. Coord. Chem.* **25** (1992) 75–84.
52. Z. Longguan, S. Kitagawa, H. C. Chang, and H. Miyasaka, *Mol. Cryst. Liquid Cryst.* **342** (2000) 97–102.
53. M. R. Sundberg, R. Uggla, and M. Melnik, *Polyhedron* **15** (1996) 1157–1163.
54. E. Colacio, J. M. Dominguez Vera, R. Kivekas, J. M. Moreno, A. Romerosa, and J. Ruiz, *Inorg. Chim. Acta* **212** (1993) 115–121.
55. A. Rodriguez-Fortea, P. Alemany, S. Alvarez, and E. Ruiz, *Chem., Eur. J.* **7** (2001) 627–637.
56. E. J. L. McInnes, F. E. Mabbs, C. M. Grant, P. E. Y. Milne, and R. E. P. Winpenny, *J. Chem. Soc., Faraday Trans.* **92** (1996) 4251–4256.

57. D. M. L. Goodgame, Y. Nishida, and R. E. P. Winpenny, *Bull. Chem. Soc. Jpn.* **59** (1986) 344–346.
58. G. A. van Albada, I. Mutikainen, U. Turpeinen, and J. Reedijk, *Polyhedron* **25** (2006) 3278–3284.
59. H. H. Monfared, Z. Kalantari, M. A. Kamyabi, and C. Janiak, *Z. Anorg. Allg. Chem.* **633** (2007) 1945–1948.
60. D. Valigura, J. Moncol, M. Korabik, Z. Pucekova, T. Lis, J. Mrozinski, and M. Melnik, *Eur. J. Inorg. Chem.* (2006) 3813–3817.
61. S. Cakir, I. Bulut, and K. Aoki, *J. Chem. Crystallogr.* **33** (2003) 875–884.
62. J. Moncol, M. Mudra, P. Lonnecke, M. Hewitt, M. Valko, H. Morris, J. Svorec, M. Melnik, M. Mazur, and M. Koran, *Inorg. Chim. Acta* **360** (2007) 3213–3225.
63. A. Doyle, J. Felcman, M. T. D. Gambardella, C. N. Verani, and M. L. B. Tristao, *Polyhedron* **19** (2000) 2621–2627.
64. T. R. Lomer and K. Perera, *Acta Crystallogr. B* **30** (1974) 2912–2913.
65. T. R. Lomer and K. Perera, *Acta Crystallogr. B* **30** (1974) 2913–2915.
66. N. E. Ghermani, C. Lecomte, C. Rapin, P. Steinmetz, J. Steinmetz, and B. Malaman, *Acta Crystallogr. B* **50** (1994) 157–160.
67. M. Kishita, M. Inoue, and M. Kubo, *Inorg. Chem.* **3** (1964) 237–242.
68. J. Mrozinski and E. Heyduk, *J. Coord. Chem.* **13** (1984) 291–298.
69. V. V. Gavrilov, Y. V. Yablokov, L. N. Milkova, and A. V. Ablov, *Phys. Status Solidi B* **45** (1971) 603–610.
70. F. P. W. Agterberg, H. Kluit, W. L. Driessen, H. Oevering, W. Buijs, M. T. Lakin, A. L. Spek, and J. Reedijk, *Inorg. Chem.* **36** (1997) 4321–4328.
71. E. Escriva, J. Server Carrio, L. Lezama, J. V. Folgado, J. L. Pizarro, R. Ballesteros, and B. Abarca, *J. Chem. Soc., Dalton Trans.* (1997) 2033–2038.

SAŽETAK

Strukturna analiza serije koordinacijskih spojeva bakra(II) i korelacija s njihovim magnetskim svojstvima

Bojan Kozlevčar i Primož Šegedin

Kemija bakra(II) u literaturi je dobro opisana zahvaljujući njenom značenju u različitim istraživačkim područjima i relativnoj lakoći priprave novih spojeva. Magnetokemija je jedno od tih područja, iako rezultati »magnetskih metoda« kao što su EPR ili magnetska susceptibilnost često ne omogućuju bolje tumačenje svojstava ovih spojeva i često su dvosmisleni. Korelacija rezultata strukturne i magnetske analize kompleksa bakra(II) može ispuniti neke od praznina u ovom području. U radu se razmatra serija kompleksa bakra(II) priređenih u našem laboratoriju, zadnjih desetak godina.